Translational molecular pathology of myxoid liposarcoma and leiomyosarcoma of soft tissue

Graaff, M.A. de

Chapter 3

A translocation t(6;14) in two cases of leiomyosarcoma: Molecular cytogenetic and array based comparative genomic hybridization characterization.

Marieke A. de Graaff, Daniëlle de Jong, Inge H. Briaire-de Bruijn, Pancras C.W. Hogendoorn, Judith V.M.G. Bovée, Károly Szuhai

Cancer Genetics. 2015; 208(11): 537-544.

Abstract

Leiomyosarcomas are malignant mesenchymal tumors recapitulating smooth muscle cell differentiation. Tumors are characterized by a genetic heterogeneity with complex karyotypes without a tumor-specific genetic aberration. Their pathobiology is still poorly understood and no specific targeted treatment is currently available for these aggressive tumors. For six leiomyosarcomas cells were cultured and analyzed by COBRA-FISH karyotyping. A t(6;14)(p;q) was identified in two cases. FISH breakpoint mapping of case L1339 reveals a breakpoint at chromosome 6p21.31 close to *HMGA1* and a small deletion was observed on the distal side of the gene. A small homozygous deletion was also found in the breakpoint region of chromosome 14q24.1 involving *ACTN1*. The second case revealed a der(6) t(6;14)(p21.1;q21.3), with a duplication adjacent to the breakpoint at chromosome 6. Confirmatory FISH revealed a second leiomyosarcoma with an aberration at 14q24.1. Alterations at this locus are found in 5% (2/39) of the leiomyosarcomas in this study. The other identified breakpoints appear to be non-recurrent, as they were not detected in other leiomyosarcomas, uterine leiomyomas, undifferentiated spindle cell sarcomas or undifferentiated pleomorphic sarcomas.

Keywords:
Leiomyosarcoma, soft tissue sarcoma, translocation, FISH, array-CGH, HMGA1.

Introduction

Leiomyosarcomas are malignant tumors originating from smooth muscle cells and responsible for 10-15% of adult soft tissue sarcomas. Tumors show a varying degree of smooth muscle differentiation which is inversely proportional to tumor grade. Histologically low grade tumors are composed of sharply demarcated bundles of spindle cells intersecting at right angles, whereas high grade lesions might contain poorly differentiated regions with nuclear pleomorphism and atypical mitoses. Areas of myxoid change, epithelioid morphology, fibrosis, hemorrhage or necrosis can be present. Smooth muscle differentiation can be detected with desmin and h-caldesmon immunohistochemistry. The retroperitoneum is the most common location but the large blood vessels, with a predilection for the vena cava inferior, the uterus and other soft tissue sites as the lower extremities are also frequently involved [1]. Lesions of the retroperitoneum and blood vessels are encountered more frequently in women; no gender predilection is present for other soft tissue locations. Leiomyosarcomas are responsible for a substantial morbidity and mortality since they are characterized by aggressive behavior, with a 5-year overall survival (OS) of 64% [2;3]. A high tumor grade, deep tumor location and large tumor size (>5 cm) were independent adverse prognostic factors for metastatic disease and overall survival [2-4]. Wide surgical excision remains the mainstay of treatment often in combination with radiation or conventional chemotherapy. No specific targeted treatment against leiomyosarcomas is at the moment available as the pathophysiology remains still poorly understood [5].

Genetically leiomyosarcomas are characterized by complex karyotypes with numerous reported non-recurrent and non-specific aberrations which result from a high degree of genetic instability [1;6;7]. Although gains and losses of many different chromosomes have been reported and the inter-tumor heterogeneity is extensive, also some similarities are described. Both cytogenetic and array-based comparative genomic hybridization (array-CGH) analyses have revealed recurrent involvement of losses of 1p, 2p, 10q, 11q, 13q, 16q and 17p and gains of 17q and 17p [2;8]. The main objective of this study is to investigate the genetic alterations in leiomyosarcomas and to search for a common molecular genetic aberration in order to improve the understanding of this malignant tumor and to identify prognostic factors or candidate targets for future therapeutic regimens. We identified two cases with t(6;14) by using

state-of-the-art molecular karyotyping tools and fine mapped breakpoint regions were tested on a tissue microarray (TMA) consisting of a large panel of leiomyosarcomas, uterine leiomyomas, undifferentiated spindle cell sarcomas and undifferentiated pleomorphic sarcomas using interphase fluorescence *in situ* hybridization (FISH).

Materials and Methods

Cell culture and COBRA-FISH

Tumor specimens were collected directly after surgery and manually dissected in small fragments. After the addition of IMDM, supplemented with 10% FBS and 1% penicillin/streptomycin (Gibco, Life Technologies, Bleiswijk, The Netherlands), they were placed in a humidified 5% CO_2 incubator at 37°C. Cells were cultured for several passages and harvested after 25 min incubation with Calyculin A (Sigma-Aldrich, Zwijndrecht, The Netherlands). Subsequently cells were placed in a hypotonic 0.075 M KCl solution followed by three fixation steps of methanol/glacial acetic acid (4:1). Slides with metaphase spreads were made in a conditioned chamber (25°C, 50% humidity; Thermotron, Holland, MI, USA).

Combined binary ratio labeling fluorescence *in situ* hybridization (COBRA-FISH) karyotyping was performed on slides with metaphase spreads of six leiomyosarcomas, no conventional G-banding studies were performed. A detailed protocol on the pre- and post-hybridization treatments has been published earlier [9]. A DMRA (Leica Microsystems, Rijswijk, The Netherlands) fluorescence microscope was used to capture images, which were analyzed with the in house developed software tool ColorProc (LUMC, Leiden, The Netherlands). Karyotypes were described according to the International System for Human Cytogenetic Nomenclature (ISCN, 2013)[10]. In three leiomyosarcomas no detectable cytogenetic abnormalities were found in the analyzed cells. Tumor cells and fibroblasts show a similar, spindle cell morphology *in vitro,* thereby making it difficult to discriminate them morphologically. The leiomyosarcomas with a seemingly normal karyotype might have contained a mix in which fibroblast have overgrown the tumor cells, these three cases are therefore excluded for further analysis.

FISH breakpoint mapping

Two-color FISH was performed to investigate the exact breakpoints of chromosomes 6p and 14q of two selected leiomyosarcoma cases. To detect possible rearrangements of the region of *HMGA1* on chromosome 6p21 bacterial artificial chromosomes (BAC) clones, RP3-349A12, proximal to the breakpoint, and RP11-936A3, distal to the breakpoint, were selected. BAC clones used in the fine mapping of the deletion breakpoints on chromosome 6 are RP11-175A, RP5-1077I5, RP3-468B3 and RP11-974K1. On region 14q24, around the *ACTN1* gene, RP11-204K16 was selected proximal and BAC clone RP11-486O13 was located distal from the breakpoint. Other BAC clones used in the fine mapping of the breakpoint on chromosome 14 are RP11-226F19 and RP11-565I3. All BAC clones were obtained from Wellcome Trust, Sanger Institute. Probes were directly labeled with FITC or Cy3 using nick translation labeling reaction. Probes were hybridized overnight on metaphase slides using a protocol otherwise identical to the COBRA-FISH protocol as described above.

Table 1: Clinicopathological and COBRA-FISH karyotyping results of three leiomyosarcoma cases.

Case	Age/ Sex	Tumor grade	Tumor size (cm)	Location	Histological features	Karyotype
L1091	70/M	3	8x7x7	Gastrocnemius muscle	Myxoid	46,XY,t(6;7)(p;p) [3]/46,XY[15]*
L1339	39/F	N/A	9x7	Uterus	Regular/ Spindle cell	45,XX,der(1;13)t(1;13) (q10;q10), t(2;10) (q;q),t(6;14)(p21.31;q24.1-24.2),der(13)t(6;13) (q?;q10),-14[6]
L1814	56/F	3	10.5x5x4.3	Hamstring muscle	Epithelioid	81,XXXX,del(X)(q),der(1;10) (q10;q10),der(1)t(1;9) (p10;p?),der(3;6) (q10;p10),+der(3)t(3;17) (q10;p10),-4,der(5)t(5;8) (q10;p10)x3, t(5;16) (q;p),+der(5)t(5;16)(q;p),-6,der(6)t(6;14)(p21.1;q21.3) hsr(6)(p?), der(7) t(6;7) (q?;q?) ,i(8)(q10)x2,der(8) t(8;22)(q10;q10), der(8),der(9)t(8;9)(q;p) x2,-10,-10,-11, der(11) t(1;11) (p;p),-13,+der(14) t(8;14)(q10;q10),-15,der(15)t(15;18)(p10 ;p?),-16,-18,-18,-19,-20,-22, der(22)t (8;9;22)(q;p;q)[3]

Abbreviation: N/A (not applicable). Uterine leiomyosarcomas are not FNCLCC-graded according to the WHO.

Array-Comparative Genomic Hybridization Analysis

Genomic DNA was isolated from frozen tumor sections of the two selected cases with a Nucleospin DNA extraction protocol (Macherey-Nagel, Düren, Germany). Tumor content was confirmed to exceed 80-90% by histologic evaluation. DNA labeling and purification were done according to the BioPrime Total Genomic Labeling System (Invitrogen); labeling efficiency was calculated with a Nanodrop ND-1000 spectrophotometer measuring A_{260} (DNA), A_{550} (Cy3) and A_{649} (Cy5). Array-based comparative genomic hybridization was performed using oligonucleotide-based human genome CGH microarray 4x44 k (Agilent Technologies, Santa Clara, CA, USA) at 65°C for 40 hr. Slides were washed according to the manufacturer's protocols and scanned using a Agilent microarray scanner with a 5 µm scan resolution. Images were imported to Feature Extraction Software and Genomic Workbench (Agilent) with human reference genome and standard settings for analysis. Commercially available healthy male or female DNA (Promega, Madison, WI, USA) was used as reference DNA. Test and reference samples were hybridized as a gender mismatch to illustrate the dynamic range of hybridization at the X and Y chromosomes.

Tissue microarray

A TMA with a broad selection of soft tissue tumors diagnosed at the Department of Pathology of the Leiden University Medical Center (LUMC), was used for confirmatory FISH analysis [11]. In this study the evaluable cases included 37 leiomyosarcomas, 17 undifferentiated pleomorphic sarcomas, 4 undifferentiated spindle cell sarcomas and 4 uterine leiomyomas. The histological diagnosis of all samples was confirmed by reviewing the hematoxylin and eosin (H&E) stained slides by a specialized bone and soft tissue tumor pathologist (JVMGB, PCWH). At least one of the smooth muscle markers h-caldesmon or desmin was positive in the leiomyosarcomas. The included leiomyosarcomas were negative for HMB45, which is a marker positive in PEComas. Soft tissue sarcomas were graded according to the FNCLCC grading system as accepted by the WHO classification [1]. Exclusion criteria were pretreatment with neoadjuvant chemotherapy or radiotherapy and radiation-induced sarcomas. All samples were handled in a coded fashion and all procedures were performed according to the ethical guidelines, "Code for Proper Secondary Use of Human Tissue in the Netherlands" (Dutch Federation of Medical Scientific Societies).

Confirmatory TMA FISH and scoring

Four different sets of BAC clones were used to screen the samples on the tissue microarray for a recurrent breakpoint as that of the two index cases (Supplementary Table 1). For the interphase FISH on TMA sections probes were labeled with biotin-dUTP or digoxigenin-dUTP using a nick translation labeling reaction. Biotin and digoxigenin labeled probes were visualized by indirect detection with Cy3-labeled streptavidin (1:500; Sigma), FITC-labeled mouse antidigoxigenin antibody (1:250; Sigma) and FITC-labeled rabbit anti-mouse antibody (1:1000; Sigma). A detailed protocol of two-color FISH on formalin-fixed, paraffin-embedded (FFPE) tissue sections has been published previously [12]. For digital archiving and annotation, all slides used for various staining procedures were scanned with the Pannoramic MIDI scanner (3DHistech, Budapest, Hungary) using brightfield or fluorescent settings for H&E sections or interphase FISH staining, respectively. Scanned images were visualized using the Pannoramic Viewer (v15.0), scoring was performed visually. For the TMA slides, at least 50 nuclei were evaluated per core with retained tissue and good signals.

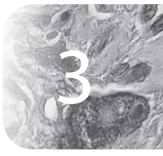

Results

Clinicopathological data and COBRA-FISH karyotyping

In this study cultured tumor cells from three leiomyosarcoma patients were suitable for cytogenetic analysis. Two patients were diagnosed with a high grade, grade 3 according to the FNCLCC grading system, leiomyosarcoma of soft tissue located in the muscles of the lower limb. One patient presented with a uterine leiomyosarcoma, which was staged according to the FIGO criteria [13;14]. All tumors expressed desmin using immunohistochemistry (Table 1).

The uterine leiomyosarcoma L1339 harbored a diploid karyotype with translocations involving several chromosomes: 45,XX,der(1;13)t(1;13)(q10;q10),t(2;10),t(6;14)(p21.31;q24.1-24.2),der(13)t(6;13)(q?;q10),-14[6]. Soft tissue leiomyosarcoma L1814 displayed a complex, hypotetraploid karyotype with multiple chromosomal rearrangements and whole chromosome gains and losses: 81,XXXX,del(X)(q),der(1;10)(q10;q10),der(1)t(1;9)(p10;p?),der(3;6)(q10;p10),+der(3)t(3;17)(q10;p10),-4,der(5)t(5;8)(q10;p10)x3,t(5;16)(q;p),+der(5)t(5;16)(q;p),-6,der(6)t(6;14)(p21.1;q21.3)hsr(6)(p?),der(7)t(6;7)

(q?;q?),i(8)(q10)x2,der(8)t(8;22)(q10;q10),der(8),der(9)t(8;9)(q;p)x2,-10,-10,-11,der(11)t(1;11)(p;p),-13,+der(14)t(8;14)(q10;q10),-15,der(15)t(15;18)(p10;p?),-16,-18,-18,-19,-20,-22,der(22)t(8;9;22)(q;p;q)[3] (Figure 1).

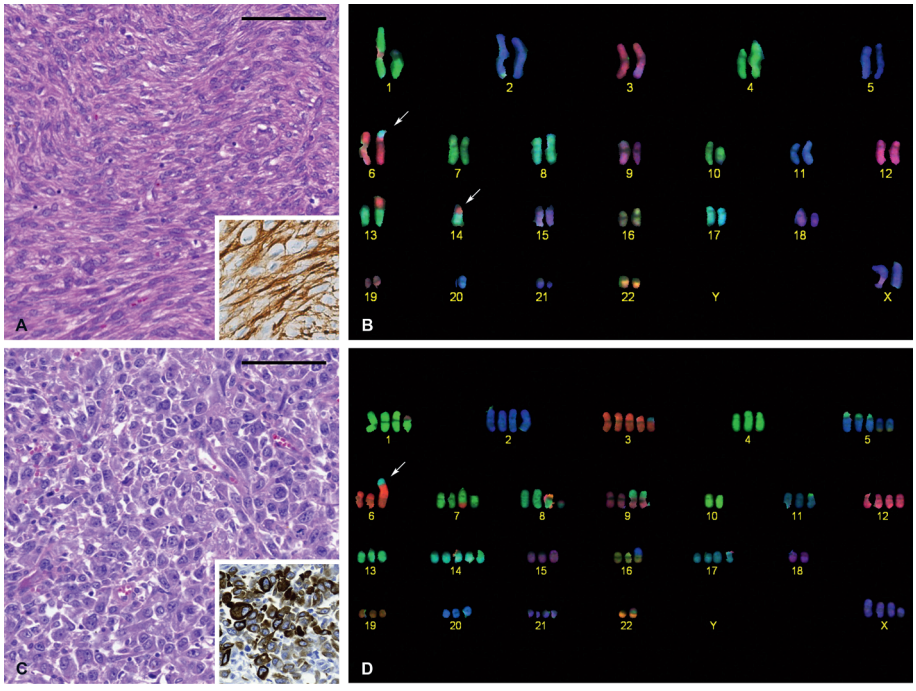

Figure 1. Histology and molecular cytogenetic results of two leiomyosarcoma cases.

H&E stained section of uterine leiomyosarcoma L1339 showing intersecting bundles of spindle cells, inset shows immunoreactivity for h-caldesmon, scale bar represents 100 µm (A). COBRA-FISH karyotype of L1339, the balanced t(6;14)(p21.31;q24.1-24.2) is indicated with white arrows (B). H&E stained section of grade 3 leiomyosarcoma L1814 with nuclear pleomorphism and multiple mitotic figures. Tumor cells exhibit epithelioid morphology with eosinophilic cytoplasm, inset shows a focal strong positive desmin staining (C). Hypotetraploid karyotype of L1814 with several translocations, including the der(6)t(6;14)(p21.1;q21.3) indicated by an arrow (D).

FISH breakpoint mapping and array-CGH profile

A seemingly balanced translocation was observed in case L1339. The breakpoint regions on chromosomal arms 6p and 14q were compatible with translocation breakpoint regions described in uterine leiomyoma involving the *HMGA1* and the *RAD51L1* genes on chromosome 6 and chromosome 14, respectively [15]. FISH mapping of the translocation regions was performed using probe sets depicted in Figure 2. Clones RP3-349A12 and RP11-936A3, proximal of and partly overlapping with the *HMGA1* locus respectively, demonstrated a split

apart in which the RP3-349A12 signal was retained on chromosome 6 while the signal of RP11-936A3 was translocated to the derivative chromosome 14. Fine mapping of this region revealed a deletion of clones RP11-175A4 and RP3-468B3 and the retention of RP5-1077I5 and RP11-974K1 bracketing this region on chromosome 6p. Breakpoint mapping on chromosome 14 using BAC clones located proximal (RP11-204K16) and distal (RP11-486O13) to *ACTN1* on chromosome 14q24, showed split signal and the distal clone was located on the derivative chromosome 6. The mapping also revealed a homozygous deletion of clones RP11-226F19 and RP11-565I3 (Figure 2B), covering the *ACTN1* gene. As secondary rearrangements at or around translocation breakpoint regions have been observed more often, we further characterized these regions by using a high resolution array-CGH approach. The array-CGH profile of L1339 detected a 603 kb deletion on 6p21.31-21.32, located 333 kb distal of *HMGA1* without the involvement of the *HMGA1* locus itself (Figure 2A). *TAPBP* was overlapping with the last distal deleted probe and might be involved in the deletion breakpoint. No copy number alteration was identified at the translocation breakpoint proximal to *HMGA1*. On chromosome 14q24.1 a 449 kb deletion was observed involving the *ACTN1* and *WDR22* genes (Supplementary Table 2). A second, 77 kb deletion was detected inside the distal part of *RAD51L1*, close to the locus of the BAC clone RP11-204K16 which is retained to chromosome 14 in the translocation. These deletions on chromosome 14 resulted in a homozygous loss of the involved chromosomal regions as monosomy 14 was observed in all tumor cells. A 7.3 Mb region at 14q21.1-21.3 was retained based on the array-CGH and likely was inserted into one of the derivative chromosomes containing chromosome 14 as no other regions were stained by whole chromosome specific paint (wcp) probes in a confirmatory FISH test using wcp 6 and wcp 14 (data not shown). Taking this together with the FISH mapping results, a balanced translocation with complex rearrangements at translocation breakpoint regions involving the *HMGA1* and *RAD51L* loci can be concluded (Figure 2).

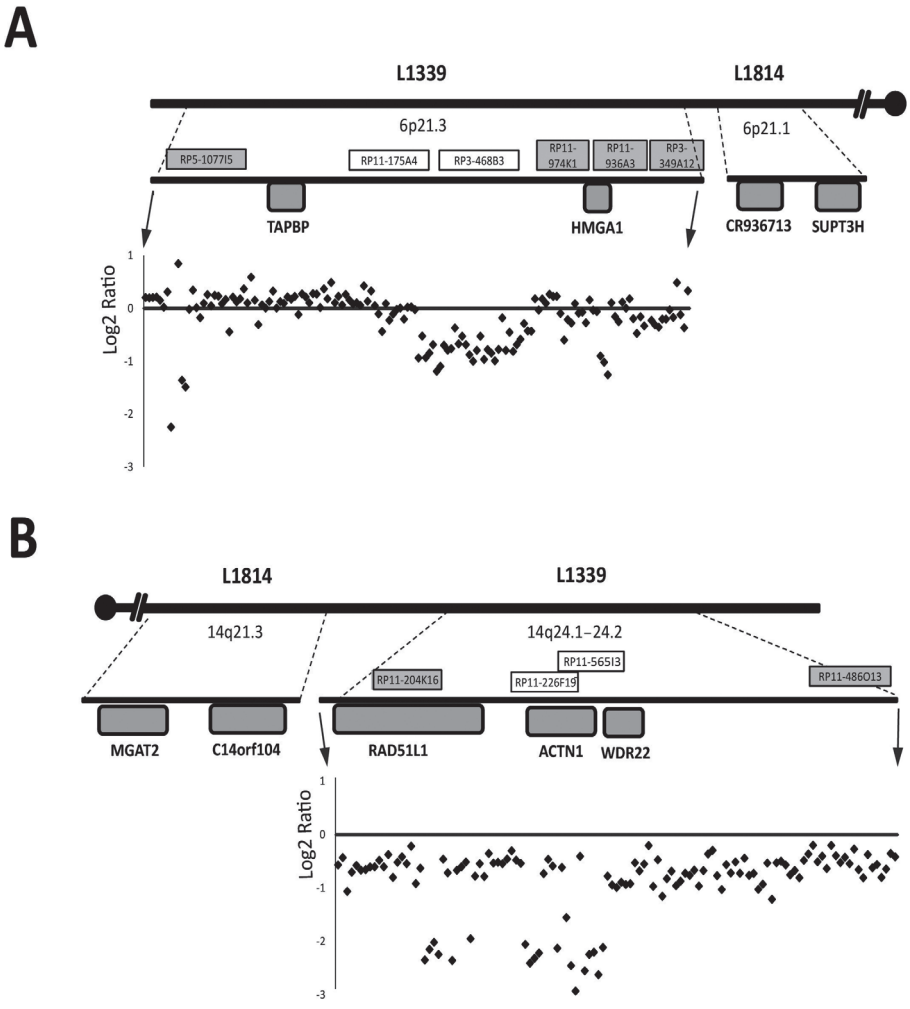

Figure 2. Schematic representation of breakpoints of leiomyosarcoma L1339 and L1814.

Schematic picture of 6p21 region with location of genes and BAC clones used for fine mapping of the translocation and deletion breakpoints of L1339; and the relation of this breakpoint compared to the breakpoint of L1814 (A). Schematic diagram of region 14q21-q24 including the genes and BAC clones involved in the translocation and deletion breakpoints (B). BAC clones in white boxes represent clones deleted in L1339, not to scale.

The hypotetraploid karyotype of L1814 resulted in a complex array-CGH profile in which the copy number varied from two to five or more of certain genomic regions. A derivative chromosome 6 involving translocations between chromosome 6 and chromosome 14 was detected. Array-CGH profiling showed

that the der(6)t(6;14) translocation was complicated with an amplification of 3.8 Mb in size at locus 6p21.1. The probes spanning the proximal breakpoint of the amplicon were 40 kb separated and *SUPT3H* was located in this region. The distance between the two probes spanning the distal amplicon breakpoint was 52 kb and was overlapping with *CR936713*. The amplification was located 6.7 Mb proximal to the *HMGA1* locus. On chromosome 14 a gain of 5.3 Mb in size was found at 14q24.2-24.3, located 3.7 Mb distal to *ACTN1*. The proximal and distal breakpoints of this gained region were spanning the *DPF3* and *ADCK1* loci, respectively. Based on the array-CGH data the translocation breakpoint was located at 14q21.3, as a slight change in copy number variation was noticed at that location. The proximal probe of the translocation breakpoint was corresponding to the *MGAT2* locus and the distal probe was overlapping with *C14orf104*. More detailed FISH-based fine mapping of the der(14)t(6;14)(p21.1;q21.3) could not be performed due to a lack of cultured tumor cells.

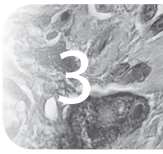

The unbalanced cytogenetic aberrations identified with COBRA-FISH were also confirmed by the array-CGH profiles of both leiomyosarcoma cases. Furthermore, the higher resolution of array-CGH revealed several other small deletions and gains in both cases.

Validation of breakpoints in other soft tissue tumors

A TMA with several soft tissue tumors was used to investigate the recurrence of the aberrations by using interphase FISH of four BAC clone sets corresponding to the regions of *HMGA1* at 6p21.31, *TAPBP* at 6p21.32, the amplicon at 6p21.1 and *ACTN1* at 14q24 (Supplementary Table 1). The two index cases were also present on the TMA and a split apart at the *HMGA1* and *ACTN1* locus and a deletion around *TAPBP* was confirmed in L1339. L1814 harbored numerous copies of BAC clone RP11-501I18 at 6p21.1, 2 Mb distal from *SUPT3H*, consistent with an amplification of that particular region; the tumor cells only contain 2 to 3 copies of centromere 6, which was included as a control. The majority of the cells of one leiomyosarcoma (L1566) revealed two times co-localization of the signals of the BAC clone set bracketing *ACTN1* and two additional signals of clone RP11-486O13 distal to *ACTN1* were present indicating an unbalanced translocation of this region. In this series, alterations involving a split apart of the signals in the 1.6 Mb region at 14q24.1-24.2 were found with FISH in 5% (2/39) of all investigated leiomyosarcomas. Copy number alterations with an equal number of the red and green signals were observed in

several tumors. None of the investigated loci showed any structural alteration in any of the additional evaluable cases including 37 leiomyosarcomas, 17 undifferentiated pleomorphic sarcomas, 4 undifferentiated spindle cell sarcomas and 4 uterine leiomyomas.

Discussion

Leiomyosarcomas belong to a group of sarcomas with a complex genetic profile without a yet identified specific, known genetic aberration. The complex karyotypes of most leiomyosarcomas might merely represent tumor progression associated changes; however, a causative role of a hidden, recurrent chromosomal aberration cannot be excluded in the development of these malignancies. In this study COBRA-FISH karyotyping of three tumors revealed a translocation t(6;14)(p;q) in two unrelated cases.

In case L1339 *HMGA1* might be involved in the breakpoint. HMGA proteins are evolutionary conserved members of the heterogeneous high-mobility group family of non-histone DNA binding proteins, they bind in the minor groove to AT-rich DNA sequences and regulate gene transcription by affecting the promotor activity and influencing the accessibility of transcription factors to target genes. They are involved in the differentiation and proliferation of mesenchymal tissues during embryonic development [16]. Some lipomas, angiomyxomas and uterine leiomyomas harbor a translocation involving *HMGA2,* at 12q15, leading to a chimeric fusion product with different partners [15;17-19]. Translocations involving *HMGA1* are identified in a subset of lipomas and uterine leiomyomas including benign uterine metastasizing leiomyoma, resulting in an upregulated expression of the chimeric protein [16;20-22]. Elevated expression has been encountered in synovial sarcoma and malignant peripheral nerve sheath tumor and is correlated with increased tumor grade and poor prognosis [23;24]. The molecular mechanism is considerably complex, as overexpression of wild type HMGA leads to deregulation of the cell cycle machinery and apoptosis in normal cells [25], while overexpression in immortalized cells stimulates tumor development [26]. The leiomyosarcomas in this study showed no intragenic *HMGA1* involvement, but a transregulatory effect due to the complex rearrangements cannot be excluded. Previously published benign mesenchymal tumors with *HMGA1* translocations mostly

revealed a break at the 3'-end, instead of an intragenic break; the breakpoint in L1339 is located less than 428 kb from the 3'-end. It has been postulated that transcriptional upregulation due to the genomic rearrangement is able to induce tumor formation [20]. Similarly complex rearrangements, involving regulatory sequences upstream of the coding sequence, have been described recently in chondromyxoid fibromas [27].

FISH mapping showed that the breakpoint at 14q24.1 in case L1339 was located at the *ACTN1* (α-actinin-1) locus, which is, like other cytoskeletal proteins, a member of the spectrin superfamily. This isoform is mainly expressed in non-muscular cells and regulates the role of focal adhesions and stress fibers and the association with cell motility [28]. High resolution array-CGH, showed a homozygous deletion of the *ACTN1* gene, which might be relevant for tumorigenesis. *RAD51L1*, located less than 200 kb to the 14q24 breakpoint, has been identified as a fusion partner of *HMGA2* in leiomyomas [15;29]. It is part of the homologous recombination repair machinery of double-strand DNA breaks. Although FISH mapping showed that the probe overlapping with *RAD51L1* was still retained to chromosome 14, array-CGH revealed a small intragenic deletion indicating a more complex rearrangement at the translocation breakpoint region with involvement of *RAD51L1*. In this way both fusion and a truncated protein expression might be possible, like mono-allelic knockout of the uterus-specific RAD51L1-11c splice variant as described in leiomyomas [30]. A uterine leiomyoma from a pseudo-Meigs' syndrome patient harbored a fast growing subclone with a deletion of the second *RAD51L1* allele next to the *RAD51L1/HMGA2* fusion [31]. Due to the monosomy 14, L1339 also has no normal copies of the gene left; the importance for tumor progression remains uncertain. Recently *RAD51L1* gene fusions were found in three uterine PEComas, it is interesting that these different mesenchymal tumors share involvement of the same gene [32]. Further research needs to be done to elucidate whether there is a common pathogenetic mechanism in the early development of these tumors. However, in our cases PEComa was excluded using immune-histochemical markers.

In L1814 a duplication at 6p21.1 was complicating the translocation breakpoint, forming the der(6)t(6;14)(p21.1;q21.3). These breakpoints differ from those in L1339. Confirmatory FISH on a TMA revealed a second leiomyosarcoma with an aberration at 14q24.1, however without involvement of the investigated regions on chromosome 6. In this study, alterations at

genomic region 14q24.1 were identified in 5% of the leiomyosarcomas. None of the other alterations appeared to be recurrent in the investigated soft tissue tumors. Nevertheless, an influence of cryptic rearrangements around *HMGA1, ACTN1* or *RAD51L1* cannot be excluded completely as they are expressed in smooth muscle cells and play a role in the development of these tumors.

Both cases harbored several other structural chromosomal aberrations, but as no other recurrent translocation was identified, these were not further investigated. In one case (L1091) we detected a balanced t(6;7)(p;p), the breakpoint region on chromosome 6 might be compatible with the *HMGA* locus. The breakpoint on chromosome 7p is different from the regions described in earlier studies [21]. However, as we had no access to more tumor cells, FISH mapping experiments could not be performed on this case. The quite simple karyotype is remarkable for a high grade leiomyosarcoma, but in the Mitelman Database of Cancer 9 out of the 129 reported cases showed a similarly simple translocation indicating a genetic subtype of leiomyosarcoma. None of the reported cases had translocation breakpoints similar to the one observed by us [33]. The case was included on the TMA, but unfortunately few cells were left with good signals so this case was not eligible for scoring.

With the currently available techniques it is challenging to identify common aberrations in these genetically heterogeneous and instable tumors. Improvements in the field of next generation sequencing have led to an increased possibility to detect aberrations. Whole-genome sequencing of osteosarcomas, a genomically complex and instable bone sarcoma, has recently shown that tumors undergo chromothripsis, leading to numerous genomic rearrangements due to reshuffling of small chromosome segments probably during a crisis-phase [34]. Chromothripsis is also found in 42% of uterine leiomyomas and it has been postulated that similar events occur during the development of leiomyosarcomas [35]. Modern sequencing techniques might be helpful to identify pathogenetic mechanisms responsible for the development of these tumors. Amplification of myocardin (*MYOCD*) at 17p is frequently encountered in leiomyosarcomas [36]. Some genetic alterations are found in only a subset of tumors indicating that they might be secondary rather than the causative, tumor initiating event. Recently mutations in dystrophin (*DMD*) have been identified in high grade mesenchymal tumors with certain level of muscle differentiation, including leiomyosarcomas, rhabdomyosarcomas and gastrointestinal stromal tumors [37]. In that study a

high percentage of the tumors has aberrations in *DMD*, suggesting that these different tumors might develop via a similar way. It will be interesting to study the role of *DMD* as deregulation of this gene might play a role in the early tumorigenesis of myogenic sarcomas.

This study reports the identification of a t(6;14)(p;q) in two leiomyosarcoma cases. As the translocation breakpoints differ, a common driver alteration for leiomyosarcomas was not found which is consistent with the genetic heterogeneity of these tumors. However, we identified genes that might be involved in the pathogenesis of these particular leiomyosarcoma cases. In the future, next generation sequencing can be a helpful tool in the search for a common driver alteration of these malignant tumors.

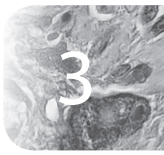

Acknowledgements
The authors would like to thank Marja van der Burg for the excellent technical assistance.

References

1. Lazar AJ, Evans HL, Shipley J. Smooth-muscle tumours. In: Fletcher CDM, Bridge JA, Hogendoorn PCW, Mertens F, editors. WHO Classification of Tumors of Soft Tissue and Bone, Lyon: IARC, 2013; pp. 109-113.
2. Italiano A, Lagarde P, Brulard C, Terrier P, Lae M, Marques B, Ranchere-Vince D, Michels JJ, Trassard M, Cioffi A, Piperno-Neumann S, Chevreau C, Blay JY, Delcambre C, Isambert N, Penel N, Bay JO, Bonvalot S, Le CA, Coindre JM, Chibon F. Genetic profiling identifies two classes of soft-tissue leiomyosarcomas with distinct clinical characteristics. Clin Cancer Res 2013;19:1190-1196.
3. Svarvar C, Bohling T, Berlin O, Gustafson P, Folleras G, Bjerkehagen B, Domanski HA, Sundby HK, Tukiainen E, Blomqvist C. Clinical course of nonvisceral soft tissue leiomyosarcoma in 225 patients from the Scandinavian Sarcoma Group. Cancer 2007;109:282-291.
4. Gladdy RA, Qin LX, Moraco N, Agaram NP, Brennan MF, Singer S. Predictors of survival and recurrence in primary leiomyosarcoma. Ann Surg Oncol 2013;20:1851-1857.
5. Radaelli S, Stacchiotti S, Casali PG, Gronchi A. Emerging therapies for adult soft tissue sarcoma. Expert Rev Anticancer Ther 2014.
6. Corless CL, Barnett CM, Heinrich MC. Gastrointestinal stromal tumours: origin and molecular oncology. Nat Rev Cancer 2011;11:865-878.
7. Hirota S, Isozaki K, Moriyama Y, Hashimoto K, Nishida T, Ishiguro S, Kawano K, Hanada M, Kurata A, Takeda M, Muhammad TG, Matsuzawa Y, Kanakura Y, Shinomura Y, Kitamura Y. Gain-of-function mutations of c-kit in human gastrointestinal stromal tumors. Science 1998;279:577-580.
8. Sandberg AA. Updates on the cytogenetics and molecular genetics of bone and soft tissue tumors: leiomyosarcoma. Cancer Genet Cytogenet 2005;161:1-19.
9. Szuhai K, Tanke HJ. COBRA: combined binary ratio labeling of nucleic-acid probes for multi-color fluorescence in situ hybridization karyotyping. Nat Protoc 2006;1:264-275.
10. ISCN (2013): An International System for Human Cytogenetic Nomenclature. Basel: S. Karger, 2013.
11. de Graaff MA, Cleton-Jansen AM, Szuhai K, Bovee JV. Mediator complex subunit 12 exon 2 mutation analysis in different subtypes of smooth muscle tumors confirms genetic heterogeneity. Hum Pathol 2013;44:1597-1604.
12. Rossi S, Szuhai K, Ijszenga M, Tanke HJ, Zanatta L, Sciot R, Fletcher CD, Dei Tos AP, Hogendoorn PC. EWSR1-CREB1 and EWSR1-ATF1 fusion genes in angiomatoid fibrous histiocytoma. Clin Cancer Res 2007;13:7322-7328.
13. Giuntoli RL, Lessard-Anderson CR, Gerardi MA, Kushnir CL, Cliby WA, Metzinger DS, Gostout BS. Comparison of current staging systems and a novel staging system for uterine leiomyosarcoma. Int J Gynecol Cancer 2013;23:869-876.
14. D'Angelo E, Prat J. Uterine sarcomas: a review. Gynecol Oncol 2010;116:131-139.
15. Dal Cin P, Quade BJ, Weremowicz S, Morton CC, Pauwels P, Van den Berghe H. Primary parauterine leiomyoma with a t(6;14). Genes Chromosomes Cancer 1999;26:385-386.
16. Reeves R. Molecular biology of HMGA proteins: hubs of nuclear function. Gene 2001;277:63-81.
17. Kazmierczak B, Pohnke Y, Bullerdiek J. Fusion transcripts between the HMGIC gene and RTVL-H-related sequences in mesenchymal tumors without cytogenetic aberrations. Genomics 1996;38:223-226.
18. Rawlinson NJ, West WW, Nelson M, Bridge JA. Aggressive angiomyxoma with t(12;21) and HMGA2 rearrangement: report of a case and review of the literature. Cancer Genet Cytogenet 2008;181:119-124.
19. Petit MM, Schoenmakers EF, Huysmans C, Geurts JM, Mandahl N, Van de Ven WJ. LHFP, a novel translocation partner gene of HMGIC in a lipoma, is a member of a new family of LHFP-like genes. Genomics 1999;57:438-441.
20. Kazmierczak B, Dal CP, Wanschura S, Borrmann L, Fusco A, Van den Berghe H, Bullerdiek J. HMGIY is the target of 6p21.3 rearrangements in various benign mesenchymal tumors. Genes Chromosomes Cancer 1998;23:279-285.
21. Nucci MR, Drapkin R, Dal CP, Fletcher CD, Fletcher JA. Distinctive cytogenetic profile in benign metastasizing leiomyoma: pathogenetic implications. Am J Surg Pathol 2007;31:737-743.

22. Bowen JM, Cates JM, Kash S, Itani D, Gonzalez A, Huang D, Oliveira A, Bridge JA. Genomic imbalances in benign metastasizing leiomyoma: characterization by conventional karyotypic, fluorescence in situ hybridization, and whole genome SNP array analysis. Cancer Genet 2012;205:249-254.
23. Hui P, Li N, Johnson C, De W, I, Sciot R, Manfioletti G, Tallini G. HMGA proteins in malignant peripheral nerve sheath tumor and synovial sarcoma: preferential expression of HMGA2 in malignant peripheral nerve sheath tumor. Mod Pathol 2005;18:1519-1526.
24. Reeves R. Nuclear functions of the HMG proteins. Biochim Biophys Acta 2010;1799:3-14.
25. Fedele M, Pierantoni GM, Berlingieri MT, Battista S, Baldassarre G, Munshi N, Dentice M, Thanos D, Santoro M, Viglietto G, Fusco A. Overexpression of proteins HMGA1 induces cell cycle deregulation and apoptosis in normal rat thyroid cells. Cancer Res 2001;61:4583-4590.
26. Wood LJ, Mukherjee M, Dolde CE, Xu Y, Maher JF, Bunton TE, Williams JB, Resar LM. HMG-I/Y, a new c-Myc target gene and potential oncogene. Mol Cell Biol 2000;20:5490-5502.
27. Nord KH, Lilljebjorn H, Vezzi F, Nilsson J, Magnusson L, Tayebwa J, de JD, Bovee JV, Hogendoorn PC, Szuhai K. GRM1 is upregulated through gene fusion and promoter swapping in chondromyxoid fibroma. Nat Genet 2014;46:474-477.
28. Sjoblom B, Salmazo A, Djinovic-Carugo K. Alpha-actinin structure and regulation. Cell Mol Life Sci 2008;65:2688-2701.
29. Schoenmakers EF, Huysmans C, Van de Ven WJ. Allelic knockout of novel splice variants of human recombination repair gene RAD51B in t(12;14) uterine leiomyomas. Cancer Res 1999;59:19-23.
30. Schoenmakers EF, Bunt J, Hermers L, Schepens M, Merkx G, Janssen B, Kersten M, Huys E, Pauwels P, Debiec-Rychter M, van Kessel AG. Identification of CUX1 as the recurrent chromosomal band 7q22 target gene in human uterine leiomyoma. Genes Chromosomes Cancer 2013;52:11-23.
31. Amant F, Debiec-Rychter M, Schoenmakers EF, Hagemeijer-Hausman A, Vergote I. Cumulative dosage effect of a RAD51L1/HMGA2 fusion and RAD51L1 loss in a case of pseudo-Meigs' syndrome. Genes Chromosomes Cancer 2001;32:324-329.
32. Agaram NP, Sung YS, Zhang L, Chen CL, Chen HW, Singer S, Dickson MA, Berger MF, Antonescu CR. Dichotomy of Genetic Abnormalities in PEComas With Therapeutic Implications. Am J Surg Pathol 2015;39:813-825.
33. Mitelman, F., johansson, B., and Mertens, F. Mitelman Database of Chromosome Aberrations and Gene Fusions in Cancer (2015). http://cgap.nci.nih.gov/Chromosomes/Mitelman .
34. Stephens PJ, Greenman CD, Fu B, Yang F, Bignell GR, Mudie LJ, Pleasance ED, Lau KW, Beare D, Stebbings LA, McLaren S, Lin ML, McBride DJ, Varela I, Nik-Zainal S, Leroy C, Jia M, Menzies A, Butler AP, Teague JW, Quail MA, Burton J, Swerdlow H, Carter NP, Morsberger LA, Iacobuzio-Donahue C, Follows GA, Green AR, Flanagan AM, Stratton MR, Futreal PA, Campbell PJ. Massive genomic rearrangement acquired in a single catastrophic event during cancer development. Cell 2011;144:27-40.
35. Mehine M, Kaasinen E, Makinen N, Katainen R, Kampjarvi K, Pitkanen E, Heinonen HR, Butzow R, Kilpivaara O, Kuosmanen A, Ristolainen H, Gentile M, Sjoberg J, Vahteristo P, Aaltonen LA. Characterization of uterine leiomyomas by whole-genome sequencing. N Engl J Med 2013;369:43-53.
36. Perot G, Derre J, Coindre JM, Tirode F, Lucchesi C, Mariani O, Gibault L, Guillou L, Terrier P, Aurias A. Strong smooth muscle differentiation is dependent on myocardin gene amplification in most human retroperitoneal leiomyosarcomas. Cancer Res 2009;69:2269-2278.
37. Wang Y, Marino-Enriquez A, Bennett RR, Zhu M, Shen Y, Eilers G, Lee JC, Henze J, Fletcher BS, Gu Z, Fox EA, Antonescu CR, Fletcher CD, Guo X, Raut CP, Demetri GD, van de Rijn M, Ordog T, Kunkel LM, Fletcher JA. Dystrophin is a tumor suppressor in human cancers with myogenic programs. Nat Genet 2014;46:601-606.

Supplementary Information

Supplementary Table 1: Combinations of BAC clones used on tissue microarrays.

BAC clone	Start position	End position	Size (kb)	Locus	Labeling	Probe region	Prox-Dist probe distance
RP3-349A12 #	34810549	34943495	132.9	6p21.31	DIG	*HMGA1* (prox)	428.1 kb
RP11-936A3 #	34207886	34382491	174.6	6p21.31	BIO	*HMGA1* (dist)	
RP11-204K16 *	68753875	68924811	170.9	14q24.1	DIG	*ACTN1* (prox)	1600.5 kb
RP11-486O13 *	70525284	70729505	204.2	14q24.2	BIO	*ACTN1* (dist)	
RP11-175A4 *	33360610	33507021	146,4	6p21.31~21.32	BIO	*TAPBP* (prox)	971.1 kb
RP5-1077I5 *	32297092	32389527	92.4	6p21.2~21.32	DIG	*TAPBP* (dist)	
RP11-501I18 *	42780788	42846928	66.1	6p21.1	BIO	2 Mb distal from *SUPT3H*	18.3 Mb
Centromere 6	Centromere 6	Centromere 6		Centromere 6	DIG	Centromere 6	

#UCSC Genome Browser Feb 2009 GRCh37/hg19, *Ensembl Genome Browser GRCh37.

Supplementary Table 2: Agilent probes describing the breakpoints.

Case	Description	Details	Agilent probe	Chromosome	Genomic location#	Genes overlapping with probe location	Distance between single probes	Distance between 2 probe sets
L1339	Deletion at 6p21.3	Last normal probe	A_16_P17503364	6p21.31	33,963,393-33,963,452	none	86.9 kb	0.603 Mb
	Proximal breakpoint	First deleted probe	A_14_P113996	6p21.31	33,876,537-33,876,596	none		(size of deletion)
	Deletion at 6p21.3	Last deleted probe	A_14_P124550	6p21.32	33,273,955-33,274,014	*TABPB*	14.4 kb	
	Distal breakpoint	Next normal probe	A_14_P125596	6p21.32	33,259,603-33,259,651	*RGL2*		
	HMGA1 locus	*HMGA1* locus	A_14_P109294	6p21.31	34,209,880-34,209,939	*HMGA1*		0.333 Mb (deletion to *HMGA1*)
L1339	Retained region 14q21	Last deleted probe	A_14_P130400	14q21.1	43,137,003-43,137,062	none	113.3 kb	7.3 Mb

Supplementary Table 2: continued

Case	Description	Details	Agilent probe	Chromosome	Genomic location#	Genes overlapping with probe location	Distance between single probes	Distance between 2 probe sets
	Proximal breakpoint	First retained probe	A_14_P114243	14q21.1	43,250,347-43,250,406	none		(size of retained region)
	Retained region 14q21	Last retained probe	A_16_P02910911	14q21.3	50,530,528-50,530,587	none	21.4 kb	
	Distal breakpoint	Next deleted probe	A_16_P02910932	14q21.3	50,551,904-50,551,963	*LOC196913*		
L1339	Deletion around *ACTN1*	Last normal probe	A_16_P02937174	14q24.1	69,111,391-69,111,449	none	24.3 kb	449.1 kb
	Proximal breakpoint	First deleted probe	A_16_P20083284	14q24.1	69,135,726-69,135,785	none		(size of deletion)
	Deletion around *ACTN1*	Last deleted probe	A_16_P20084485	14q24.1	69,584,790-69,584,847	*WDR22*	39.1 kb	
	Distal breakpoint	Next normal probe	A_16_P20084596	14q24.1	69,623,872-69,623,931	none		
L1339	Deletion in *RAD51L1*	First proximal deleted probe	A_16_P20081907	14q24.1	68,655,255-68,655,314	*RAD51L1*	76.5 kb	76.5 kb
	Deletion in *RAD51L1*	Last distal deleted probe	A_16_P40226246	14q24.1	68,731,769-68,731,828	*RAD51L1*		(size of deletion)
L1814	Amplification at 6p21.1	Last normal probe	A_16_p17530102	6p21.1	44837840-44837899	*SUPT3H*	40.4 kb	3.8 Mb
	Proximal breakpoint	First amplified probe	A_14_P103947	6p21.1	44797474-44797533	*SUPT3H*		(size of amplification)
	Amplification at 6p21.1	Last amplified probe	A_16_P17520532	6p21.1	40987901-40987960	*CR936713*	51.6 kb	
	Distal breakpoint	Next normal probe	A_14_P130391	6p21.1	40936271-40936330	*CR936713*		
L1814	Translocation breakpoint	Proximal	A_14_P104481	14q21.3	50,088,698-50,088,757	*MGAT2*	6.0 kb	

Supplementary Table 2: continued

Case	Description	Details	Agilent probe	Chromosome	Genomic location#	Genes overlapping with probe location	Distance between single probes	Distance between 2 probe sets
	Translocation breakpoint	Distal	A_14_P115913	14q21.3	50,094,743-50,094,802	*C14orf104*		
L1814	Duplication at 14q24.2	Last normal probe	A_16_P02942905	14q24.2	73145087-73145146	*DPF3*	31.0 kb	5.3 Mb
	Proximal breakpoint	First duplicated probe	A_16_P02942958	14q24.2	73176127-73176186	*DPF3*		(size of duplication)
	Duplication at 14q24.2	Last duplicated probe	A_14_P132604	14q24.3	78389188-78389247	*ADCK1*	38.8 kb	
	Distal breakpoint	Next normal probe	A_16_P20105656	14q24.3	78428021-78428080	none		

#UCSC Genome Browser Feb 2009 GRCh37/hg19